Title

Characterization of an Inducible Alcoholic Liver Fibrosis Model for Hepatocellular Carcinoma Investigation in a Transgenic Porcine Tumorigenic Platform

Journal

Journal of Vascular and Interventional Radiology, 29(8)

ISSN

1051-0443

Authors

Gaba, Ron C
Mendoza-Elias, Nasya
Regan, Daniel P
et al.

Publication Date

2018-08-01

DOI

10.1016/j.jvir.2018.03.007

Peer reviewed

HHS Public Access

Author manuscript

J Vasc Interv Radiol. Author manuscript; available in PMC 2019 February 25.

Published in final edited form as:

J Vasc Interv Radiol. 2018 August ; 29(8): 1194–1202.e1. doi:10.1016/j.jvir.2018.03.007.

Characterization of an Inducible Alcoholic Liver Fibrosis Model for Hepatocellular Carcinoma Investigation in a Transgenic Porcine Tumorigenic Platform

Ron C. Gaba, MD,
Department of Radiology University of Illinois Health, 1740 West Taylor Street, MC 931, Chicago, Illinois, 60612

Nasya Mendoza-Elias, BS,
College of Medicine, University of Illinois at Chicago, Chicago, Illinois

Daniel P. Regan, DVM, PhD,
Flint Animal Cancer Center, Colorado State University, Fort Collins, Colorado

Kelly D. Garcia, DVM, PhD,
Biological Resources Laboratory, University of Illinois at Chicago, Chicago, Illinois

R. Peter Lokken, MD, MPH,
Department of Radiology, University of Illinois Health, 1740 West Taylor Street, MC 931, Chicago, Illinois, 60612

Regina M. Schwind, BS,
Department of Radiology, University of Illinois Health, 1740 West Taylor Street, MC 931, Chicago, Illinois, 60612

Michael Eichner, DVM,
Biological Resources Laboratory, University of Illinois at Chicago, Chicago, Illinois

Faith M. Thomas, BS,
Department of Animal Sciences, University of Illinois at Urbana-Champaign, Urbana and Champaign, Illinois

Lauretta A. Rund, PhD,
Department of Animal Sciences, University of Illinois at Urbana-Champaign, Urbana and Champaign, Illinois

Lawrence B. Schook, PhD, and
Department of Radiology, University of Illinois Health, 1740 West Taylor Street, MC 931, Chicago, Illinois, 60612

Department of Animal Sciences, University of Illinois at Urbana-Champaign, Urbana and Champaign, Illinois

Kyle M. Schachtschneider, PhD

Address correspondence to K.M.S. kschach2@uic.edu.

None of the authors have identified a conflict of interest

Department of Radiology, University of Illinois Health, 1740 West Taylor Street, MC 931, Chicago, Illinois, 60612

Abstract

Purpose: This study used the Oncopig Cancer Model (OCM) to develop alcohol-induced fibrosis in a porcine model capable of developing hepatocellular carcinoma.

Materials and Methods: Liver injury was induced in 8-week-old Oncopigs (n = 10) via hepatic transarterial infusion of 0.75 mL/kg ethanol-ethiodized oil (1:3 v/v). Feasibility was assessed in an initial Oncopig cohort (n = 5) by histologic analysis at 8 weeks after induction, and METAVIR results were compared to age- and sex-matched healthy controls (n = 5). Liver injury was then induced in a second OCM cohort (n = 5) for a time-course study, with post-induction disease surveillance via biweekly physical exam, lab analysis, and liver biopsies until 20 weeks after induction.

Results: In Cohort 1, 8-week post-induction liver histologic analysis revealed median METAVIR F3 (range, F3-F4) fibrosis, A2 (range, A2-A3) inflammation, and 15.3% (range, 5.0%—22.9%) fibrosis. METAVIR and inflammation scores were generally elevated compared to healthy controls (F0-F1, $P = 0.0013$; A0-A1, $P = .0013$; median percent fibrosis 8.7%, range, 5.8%—12.1%, $P = .064$). In Cohort 2, histologic analysis revealed peak fibrosis severity of median METAVIR F3 (range, F2-F3). However, lack of persistent alcohol exposure resulted in liver recovery, with median METAVIR F2 (range, F1-F2) fibrosis at 20 weeks after induction. No behavioral or biochemical abnormalities were observed to indicate liver decompensation.

Conclusions: This study successfully validated a protocol to develop METAVIR F3-F4 fibrosis within 8 weeks in the OCM, supporting its potential to serve as a model for hepatocellular carcinoma in a fibrotic liver background. Further investigation is required to determine if repeated alcohol liver injury is required to develop an irreversible METAVIR grade F4 porcine cirrhosis model.

Hepatocellular carcinoma (HCC) is a deadly tumor that accounts for more than 9% of annual cancer mortality (1,2). While global cancer incidence is generally decreasing, HCC incidence is projected to continually increase for the foreseeable future, given the growing prevalence of chronic liver diseases that cause liver cirrhosis (3). Alcoholic liver disease is a major cause of liver cirrhosis and increases the risk for hepatocarcinogenesis (4). Since the health status of the liver can also have profound effects on HCC tumor biology, treatment allocation, and response to therapy (5), a large animal model capable of exhibiting both HCC and liver cirrhosis concurrently would be a valuable resource for advancing preclinical investigation of HCC detection, development, natural history, and response to treatment in its native comorbid cirrhotic background. Although previous studies have investigated cirrhosis induction in domestic pigs (6), the applicability of induction protocols across genotypically distinct pig breeds, including those amenable to tumor development, is unknown. This study used the innovative Oncopig Cancer Model (OCM)—a transgenic porcine model that recapitulates human cancer through development of site- and cell-specific tumors via induced expression of heterozygous $KRAS^{G12D}$ and $TP53^{R167H}$ transgenes (7)—to develop alcohol-induced fibrosis in a porcine model capable of developing HCC tumors (8).

MATERIALS AND METHODS

Animal Subjects and Study Design

Work was completed at the University of Illinois at Chicago and the University of Illinois at Urbana-Champaign. Institutional Animal Care and Use Committee approval was obtained. Details of animal care are in Appendix A (available online at www.jvir.org). The study design consisted of 2 chronologically staged experiments spanning 2 successive cohorts of non-tumor-laden Oncopigs (Fig 1). Sample sizes reflected those typically used in exploratory, pilot studies (9). The first experiment aimed to validate the ability of a previously published protocol (6) to produce liver fibrosis in the OCM. In the first OCM cohort (n = 5), liver injury was induced and followed by post-induction disease surveillance via biweekly lab analysis, with subsequent euthanasia, liver harvest, and liver histologic assessment at 8 weeks after induction. Laboratory and histologic results were also compared to age- and sex-matched healthy control Oncopigs (n = 5). Liver was harvested from control animals for pathologic comparison at age-matched time points to subjects in Cohort 1. After validation of fibrosis induction in Oncopigs, the procedure was repeated for an extended time- course experiment in a second OCM cohort (n = 5) to investigate disease progression and the ability to provoke sustained liver disease. In this second OCM cohort, physical examination, lab analysis, and serial liver biopsies were obtained at 2-week intervals for 20 weeks, followed by euthanasia, liver harvest, and histologic assessment.

Study Cohort

The study cohort included 10 female Oncopigs of a median age of 57 days (range, 51–62 days) and a median weight of 14.0 kg (range, 11.7–18.2 kg) at the time of fibrosis induction. Oncopigs in Cohort 1 were significantly older (median age, 62 days; range, 60–62 days versus 54 days; range, 51–54 days; $P = .008$) and heavier (median weight, 16.2 kg; range, 15.9–18.2 kg versus 12.4 kg, range, 11.7–14.2 kg; $P = .036$) than those in Cohort 2 at the time of fibrosis induction. No significant differences were observed in biometric data between the Oncopigs in Cohort 1 and the healthy age- and sex-matched control subjects (median weight, 36.9 kg; range, 26.5–42.7 kg versus 39.0 kg; range, 35.8–40.4 kg; $P = .841$) at 16 weeks of age (corresponding to 8 weeks after induction).

Procedures

Fibrosis Induction.—All fibrosis induction procedures were performed by 1 of 2 board-certified interventional radiology (IR) physicians with 9 years of experience (R.C.G.) and 4 years of experience (R.P.L.), according to a modification of the methodology described by Avritscher et al (6). At 8 weeks of age, Oncopigs underwent anesthetic induction, followed by intubation and maintenance with 1%−3% iso- flurane. Angiography was performed using a C-arm (OEC Medical Systems series 9600; GE Healthcare, United Kingdom). With the animal supine, the groin was sterilely prepared. Ultrasound-guided vascular access was gained viathe common femoral artery with placement of a 5-French sheath (Pinnacle; Terumo Medical Corporation, Somerset, New Jersey). Using standard catheter and wire techniques, celiac arteriography was performed using a 5-French catheter (Sos Omni Selective; AngioDynamics, Latham, New York) (Fig 2). A coaxial 3-French microcatheter (Renegade Hi-flo; Boston Scientific, Marlborough, Massachusetts) was advanced into the

common hepatic artery using a micro- guidewire. Arteriography was performed with iohexol (Omnipaque-300; Amersham Health, Princeton, New Jersey). The microcatheter was then advanced into the proper hepatic artery, and 0.75 mL/kg of a 1:3 v/v emulsified mixture of absolute ethanol and ethiodized oil (Lipiodol; Guerbet, Villepinte France, used to deliver ethanol into the liver and transiently embolize the liver microcirculation) was slowly infused by hand injection over 30 minutes (Fig 2). Post-infusion arteriograms were not performed. Dosing ofthe administered ethanol and ethiodized oil emulsion was derived by dividing the 28-mL maximally tolerated dose by mean pig weight reported in the study of Avritscher et al (6). Upon completion of the infusion, all devices were removed, and hemostasis was achieved via manual compression. After induction procedures, animals were recovered, returned to their pens, and followed-up daily until sacrifice (Cohort 1) or biopsy (Cohort 2).

Liver Biopsy.—Percutaneous ultrasound-guided liver biopsy procedures were performed by a board-certified IR physician with 9 years of experience (R.C.G.), a board- certified laboratory animal veterinarian with 20 years of experience (K.D.G.), a veterinarian with 2 years of experience (M.E.), or a medical student research associate (N.M.E.) under the direct supervision of 1 of these 3 practitioners; the same operator did not necessarily perform all biopsies for a given animal. Liver biopsies were undertaken in a surgical suite after animal subject intubation and maintenance under general anesthesia. With the animal supine, the abdomen was sterilely prepared. An 18-gauge automated biopsy device (BioPince; Argon Medical Devices, Plano, Texas) was then advanced into the right liver lobe (selected given favorable subcostal sonographic visibility), and 3–4 2-cm-long core specimens were sequentially obtained and transferred to a container containing 10% neutral buffered formalin for fixation. After liver biopsy, animals were recovered, returned to their pens, and followed-up daily until subsequent biopsy or sacrifice.

Clinical and Laboratory Assessment

OCM subjects in Cohort 2 underwent clinical assessment at baseline and biweekly after induction thereafter, which included evaluation for ascites via ultrasound, as well as examination for the presence of hepatic encephalopathy (HE) resulting in neurologic impairment. Clinical assessments were performed by a board-certified laboratory animal veterinarian with 20 years of experience (K.D.G.) and a medical student research associate (N.M.E.), who were not blinded to treatment. HE was determined by neurologic assessment of general appearance (quiet versus bright, alert, and responsive), cooperativity, appetite, and gait instability, as well as through a leg placement test (10).

OCM subjects in both cohorts underwent laboratory testing at baseline and biweekly after induction thereafter, which included standard blood chemistries relevant to the diagnosis and staging of chronic liver disease and pertinent for patient eligibility for locoregional therapy (LRT) for liver cancer. Laboratory evaluations included a complete blood count, total bilirubin, alkaline phosphatase, aspartate aminotransferase (AST), albumin, and prothrombin time. Laboratory testing for healthy control Oncopigs was performed at age-matched time points equivalent to 2, 4, 6, and 8 weeks after induction.

Animal Necropsy and Tissue Harvest

Euthanasia was performed at either 8 weeks (Cohort 1) or 20 weeks (Cohort 2) after induction using a lethal dose of 150-mg/kg saturated sodium pentobarbital solution (Schering-Plough, Kenilworth, New Jersey). Healthy control subjects were sacrificed at age-matched time points to Cohort 1. Necropsy was performed, and Oncopig livers were harvested in their entirety. Next, representative samples of liver tissue weighing approximately 20 g were taken from both fibrotic (Cohorts 1 and 2) and normal- appearing (Cohorts 1 and 2, and healthy control subjects) liver areas and transferred to a container containing 10% neutral buffered formalin for fixation and pathologic processing.

Histologic Processing and Analysis

Formalin-fixed liver samples were embedded in paraffin, sectioned at 4μm thickness, and mounted onto glass slides. Slides were stained using hematoxylin and eosin and Masson's trichrome. Descriptive and semiquantitative histopathologic analyses were performed by a board-certified veterinary pathologist (D.P.R.) with 6 years of experience who was blinded to the treatment arm. For analysis, whole slides were scanned using a Hamamatsu Nanozoomer scanner (Hamamatsu Photonics, Hamamatsu, Japan), and digital images were visualized with NDP.view2 software (Hamamatsu) and graded for fibrosis and inflammation according to a porcine-adapted METAVIR system (**Tables** 1, 2) (11,12). In addition, digital images of trichrome-stained slides were also imported to ImageJ (National Institutes of Health) (13) using BioFormats (14) and subjected to color deconvolution for quantification of trichrome-positive collagen, expressed as a percentage of total liver tissue section area.

Definitions, Outcome Measures, and Statistical Analysis

The primary outcome measures of this study were effectiveness and durability of fibrosis induction. Effectiveness of fibrosis induction was measured by the occurrence of F2-F4 fibrosis at any time after the procedure; durability of fibrosis was defined as the fraction of Cohort 2 cases exhibiting persistence of the most severe cirrhotic phenotype achieved in each individual Oncopig subject at 20 weeks after induction. Liver cirrhosis was defined as F4 fibrosis (12). Secondary outcome measures included technical success of fibrosis induction procedures, relative fibrosis compared to normal-appearing liver areas and healthy control liver, rate of clinical liver decompensation, and incidence of liver lab dysfunction. Technical success was defined by proper hepatic artery catheterization with delivery of the entire prescribed dose of ethanol and ethiodized oil emulsion. Clinical liver decompensation was defined by occurrence of ascites and/or HE. Liver lab dysfunction was defined by alterations in blood chemistries compared to available laboratory reference range values (10), with secondary comparison to age- and sex-matched healthy control subjects.

Statistical analyses were performed using SPSS Statistics software version 22 (SPSS Inc, Chicago, Illinois). Descriptive statistics were used to characterize features of the cohort and to quantify post-induction histologic outcomes. Values between groups were compared using the Wilcoxon- Mann-Whitney test, the Wilcoxon signed-rank test, or the Kruskal-Wallis 1-way analysis of variance test. All statistical tests were 2 sided. *P* values less than .05 were considered statistically significant.

RESULTS

Fibrosis Induction Procedures

Technical success was achieved in 9/10 (90%) cases. Although all animal subjects developed reduced arterial flow during ethanol-ethiodized oil infusion as assessed under fluoroscopy, in only 1 case in Cohort 2, stasis in the hepatic arterial circulation required early termination of ethanol and ethiodized oil emulsion after 60% of the prescribed dose was infused (6 mL emulsion infused). A median of 10 mL (range, 6–12 mL) of absolute ethanol and ethiodized oil emulsion was administered. No procedure-related complications or mortality were encountered.

Clinical and Laboratory Outcomes

Clinical examination revealed no evidence of liver decompensation. Neither ascites nor HE was evident in any porcine subject during the follow-up periods. Representative laboratory outcomes from select pre- and post-induction time points are displayed in Table 3. No abnormalities inplatelet count, total bilirubin, alkaline phosphatase, or AST were observed in alcohol-induced fibrosis (experimental) and healthy control Oncopigs compared to available laboratory reference range values. Albumin levels exceeded available laboratory reference range values in Cohort 1, Cohort 2, and healthy control porcine subjects, but baseline and week-4 values in Cohorts 1 and 2 were not different than those for healthy control subjects ($P > .05$). A statistically significant difference across week 6 albumin values (3.5 vs 3.2 vs 3.3, $P = .008$) was evident. No laboratory reference range values were available for prothrombin time, although baseline and week-4 values in Cohorts 1 and 2 were not different than those for healthy control subjects ($P > .05$). A statistically significant difference was observed across week-6 prothrombin time values (12.65 vs 12.8 vs 14.4, $P = .044$).

Pathologic Outcomes

Cohort 1.—Gross pathologic evaluation at necropsy revealed evidence of macronodular liver fibrosis that heterogeneously affected the liver, with areas of fibrosis and areas of normal-appearing liver present in all Cohort 1 Oncopigs at 8 weeks after induction (Fig 3). Histopathologic analysis of liver specimens collected at necropsy 8 weeks after induction demonstrated significant fibrosis induction in all 5 Oncopigs (Fig 4). Histologic findings in these animals were characterized by regionally extensive foci of moderate to marked fibrous expansion of both portal tracts and preexisting fibrous septa. Multifocally admixed with this fibrous tissue and infiltrating portal and septal tracts were moderate numbers of inflammatory cells composed primarily of lymphocytes and plasma cells, with fewer pigment-laden macrophages and rare eosinophils. Frequently, portal inflammation and fibrosis disrupted the limiting plate and dissected into the adjacent lobular parenchyma and often partially or completely encircled hepatic lobules, which appeared small and irregular and contained swollen hepatocytes undergoing lipid-type vacuolar degeneration.

Effectiveness of fibrosis induction in Cohort 1 was 100% (5/5) (Table 4). At 8 weeks, the METAVIR fibrosis score for fibrotic liver from experimental animals (median F3, range F2-F4) (Fig 4) was significantly higher ($P = .0013$) than normal liver from both experimental

animals (median F0, range F0-F1) and healthy control pigs (median F0, range F0-F1) (Fig 4). In addition, the inflammation score for fibrotic liver from experimental pigs (median A2, range A2- A3) was also significantly higher ($P = .0013$) than normal liver from both experimental animals (median A0, range A0-A1) and healthy control pigs (median A1, range A0- A1). Median percent fibrosis (15.3%, range 5.0%−22.9%) was elevated in comparison to normal liver from both experimental animals (median 6.1%, range 2.5% −9.4%; $P = .080$) and healthy control pigs (median 8.7%, range 5.8%-12.1%. $P = .064$) but did not reach statistical significance.

Cohort 2.—Gross pathologic evaluation demonstrated a normal appearance of the liver in all Cohort 2 Oncopigs at 20 weeks after induction. Histologic changes in these animals were similar to but less severe than those described for Cohort 1.

Effectiveness of fibrosis induction in Cohort 2 was 100% (5/5). Histopathologic examination demonstrated evidence of fibrosis as early as 2 weeks after induction (Fig 5), with a median METAVIR fibrosis score of F2 (range, F1-F3), a median inflammation score of A2 (range, A1-A2), and a median percent fibrosis of 8.1% (range, 6.6%−11.6%) at this time point. During the follow-up period, fibrosis severity peaked at median METAVIR grade F3 (range, F2- F3) and median inflammation score A2 (range, A1-A2) (Table 5), but durability of fibrosis was 0% (0/5). Twenty- week post-induction liver histologic analysis revealed a median METAVIR fibrosis score of F2 (range, F1-F2), with a reduced median inflammation score (median A1) (Table 5, Fig 5) but with a similar median percent fibrosis (8.7%, range 7.4%−10.5%). Evaluation of serial biopsy specimens from this cohort did not demonstrate histologic evidence of fibrosis progression or cirrhosis development. Some observed variation in histologic results across different time points was thought to reflect sampling variation as well as fibrosis heterogeneity (Table E1 [available online at www.jvir.org]).

DISCUSSION

The prevalence of liver cirrhosis is approximately 4.5%- 9.5% (15,16), affecting hundreds of millions of people worldwide and more than 600,000 people in the United States (17). This disease accounts for approximately 2% of all global mortality, approximating 1 million deaths per year (18). Of the causes of liver cirrhosis, alcoholic liver disease underlies approximately 20% of deaths (19). Liver cirrhosis increases the risk for development of HCC, an aggressive malignancy that spans more than 780,000 new diagnoses and 750,000 annual deaths (1,2). These staggering data highlight the urgent need for further investigation into HCC detection, development, and natural history, and response to LRT in its native comorbid cirrhotic background.

Current animal models for HCC have significant disadvantages, including limited recapitulation of the human condition and the protracted length of time required for model establishment. Moreover, most available models lack the anatomic size necessary to trial new therapies targeted toward curing human disease, and small animal HCC models have meaningful deficiencies in their ability to predict clinical outcomes (20). The transgenic OCM is a unique genotypically, anatomically, and physiologically relevant large animal model for preclinical study of human disease that develops site- and cell-specific tumors

after Cre recombinase exposure (7). The OCM was designed to harbor mutations found in more than 50% of human cancers— *KRAS*^{G12D} and *TP53*^{R167H}—which result in OCM HCC that recapitulates the phenotype and physiology of human tumors (8). As HCC develops in patients with liver cirrhosis, an ideal HCC model must also be able to reflect this comorbidity. The ability to concurrently induce liver cirrhosis and HCC in the OCM provides the opportunity to assess the role of chronic liver disease in HCC tumorigenesis. Although autochthonous HCC tumors have been developed in chemically induced porcine HCC models (21,22), such models require more than 1 year to develop clinically relevant tumors and do not allow for control of tumor number, location, or comorbidities as in the OCM, rendering them potentially less suitable for preclinical and co-clinical trials. In contrast, OCM tumor induction can theoretically occur within a 2–3-month timeframe, which aligns with the timeframe for concurrent fibrosis induction.

In the current study, a previously published protocol (6) was successfully validated and used to develop METAVIR F3-F4 fibrosis within 8 weeks in the OCM, demonstrating the reproducibility of this protocol across pig breeds. Although a significant increase in percent fibrosis was observed when comparing grossly cirrhotic and normal- appearing liver samples from experimental and control animals, this increase did not reach significance, which may reflect insufficient statistical power due to small sample size. Despite the promising results from Cohort 1, results of a prolonged time-course experiment indicated liver recovery, with METAVIR grade F1 -F2 fibrosis levels at 20 weeks after induction. These results indicate that a single infusion of ethanol and ethiodized oil induces only transient fibrosis with little inflammation and hepatocellular necrosis. This represents a significant drawback of the described induction procedure. The liver recovery observed in this study is consistent with the reversal of liver fibrosis observed in abstinent patients presenting with pre-cirrhotic alcohol-induced liver damage (23,24), with regression occurring through resorption of extracellular fibers and collagenous bundles (25). Overall, these results suggest that prolonged or repeated exposure to alcohol is required to develop a durable, irreversible METAVIR F4 large animal model of cirrhosis, with diffuse penetrance required to recapitulate the cirrhotic phenotype observed in humans. The use of multiple induction procedures may more closely mimic the repeated cycle of hepatocyte injury, inflammation, and repair that is required to induce extracellular matrix protein deposition and fibrogenesis (23). It remains unclear, however, whether the natural history of Oncopig METAVIR F4 fibrosis (cirrhosis) differs from that of METAVIR F1-F3 fibrosis in regard to regression. Because both cases of F4 fibrosis in the current study were in the 8-week sacrifice group, these results do not provide insights into cirrhosis temporal durability in the OCM.

Although liver fibrosis was observed in 100% (10/10) of induced Oncopigs, no clinically relevant liver decompensation or laboratory changes were observed over time. This result indicates that although liver damage was successfully induced, the disease was not sufficiently severe, widespread, or homogeneous to affect general health or liver function of Oncopigs. The current results contrast with those reported by Avritscher et al, who described occurrence of ascites in their porcine cirrhosis cohort (6). While seemingly discordant, these differential outcomes are in line with the concept that different individuals—in this case, Oncopig versus domestic pig—may manifest differential response to the same causative stress due to underlying genetic differences (26). It is also likely that the ethanol and

ethiodized oil dose administered in this study was less than that infused in some cases of Avritscher et al, where weight-based dosing ranged from 0.60 mL/kg to 0.95 mL/kg (6).

The lack of diffuse disease observed both grossly and histologically in the first experimental cohort herein suggests that the temporal variations in METAVIR scores observed in the second experimental cohort are likely due to collection of biopsies from liver segments with variable disease burden, given the heterogeneity of fibrotic distribution in explants. To this end, core needle biopsy may not represent the optimal approach to survey fibrosis in this model, given potential for disease heterogeneity and sampling error. In contrast, advanced radiologic imaging techniques, such as magnetic resonance elastography (MRE), may provide a more global view of the liver with capability to diagnosis fibrosis non- invasively. In humans, MRE has been shown to provide valuable qualitative and quantitative assessment of liver fibrosis (27–29). From a preclinical standpoint, Huang et al were able to demonstrate a positive correlation between liver stiffness and histologic fibrosis in an 8-pig pilot study investigating the utility of MRE in swine (11); a similar analysis using the Oncopig platform has been initiated.

This investigation had limitations. First, the sample size of Oncopigs used was small. However, the information acquired was maximized by obtaining histologic, laboratory, and clinical data from all subjects, allowing a comprehensive clinicopathologic assessment. Second, while the dosing of the administered ethanol and ethiodized oil emulsion was empiric, it was derived from a published protocol and represented a consistent weight-based dose that allows a defined starting point for developing a relationship between administered dose and fibrosis response in future investigations. Third, variation in histologic results across liver biopsies—likely due to sampling variation as well as fibrosis heterogeneity—may have underestimated and confounded interpretation of fibrosis severity over time in Cohort 2. Fourth, this study did not include measurement of hepatic venous pressure gradients to assess the occurrence of hemodynamic alterations. Fifth, this investigation did not assess the impact of anatomic effects of ethanol-ethiodized oil on the hepatic arterial vasculature. It is theoretically possible that such an emulsion could result in irreversible arterial alterations (eg, stenosis and occlusions) that could affect subsequent LRT administration; however, treatment session multiplicity in published trials of ethanol-ethiodized oil emulsion transarterial therapy of HCC suggest durable patency of the hepatic vasculature (30,31).

In conclusion, this study successfully validated a protocol to develop METAVIR F3-F4 fibrosis within 8 weeks in the OCM, supporting its potential to serve as a model for HCC in a cirrhotic liver background. However, repeated liver injury may be required to develop an irreversible METAVIR grade F4 porcine model of cirrhosis. Future investigations will investigate whether multiple transarterial infusions of an ethanol and ethiodized oil emulsion will result in development of a sustained, chronic porcine model of alcohol-induced liver cirrhosis.

Extended Data

Table E1.

Cohort 2 Biweekly Liver Histologic Outcomes

	METAVIR Fibrosis Grade and Inflammation Activity									
	Week 2	**Week 4**	**Week 6**	**Week 8**	**Week 10**	**Week 12**	**Week 14**	**Week 16**	**Week 18**	**Week 20**
Subject 1	F2, A1	F1, A0	F3, A1	F1, A0	F1, A1	F3, A1	F3, A1	F1, A1	F2, A1	F2, A1
Subject 2	F2, A2	F0, A0	_ *	F0, A1	- *	F0, A0	- *	- *	F2, A1	F2, A1
Subject 3	F2, A2	F1, A1	F2, A1	F0, A1	F1, A1	F2, A1	F2, A1	F3, A1	F1, A1	F1, A1
Subject 4	F3, A2	F2, A1	F2, A1	F1, A1	- *	- *	F2, A1	F2, A1	F1, A1	F1, A1
Subject 5	F1, A2	F3, A1	F1, A1	F0, A0	F2, A1	F3, A1	F3, A1	F2, A2	F2, A1	F2, A1

* Samples insufficient for histologic diagnosis.

ACKNOWLEDGMENTS

Histologic services were provided by the Research Resources Center Research Histology and Tissue Imaging Core at the University of Illinois at Chicago, established with the support of the Vice Chancellor of Research. The authors acknowledge Javier Sedillo, Histology Technologist in the University of Illinois Health Department of Pathology, for assistance with digitization of histologic slides used for analysis in the current study. This work was supported in part by the United States Department of Defense, Translational Team Science Award CA150590. This research has been submitted to the American Association for Cancer Research 2018 Annual meeting in Chicago, Illinois.

APPENDIX A.: ANIMAL SUBJECT CARE

The Oncopig line was maintained as a specific pathogenfree clean herd at the University of Illinois at Urbana- Champaign, and work was completed at the University of Illinois at Chicago and the University of Illinois at Urbana- Champaign. Both institutions maintain full Association for th Assessment and Accreditation of Laboratory Animal Care International (AAALAC) accreditation. Animal housing and husbandry practices were fully compliant with the 8th Edition of the Guide for the Care and Use of Labo- rafigtory Animals (National Research Council, 2011) and with the 3rd Edition of the Guide for the Care and Use of Agricultural Animals in Research (Federation of Animal Science Societies, 2010). Briefly, all animals (both experimental and control) were group-housed in an indoor facility maintained at a dry bulb temperature between 61F and 81T at 30%−70% humidity. The light cycle was kept at 12:12 light:dark (University of Illinois at Chicago) or 14:10 light:dark (University of Illinois at Urbana-Champaign). Animals had constant access to water and were fed daily. Their diet was designed by a faculty member in the Division of Nutritional Sciences at University of Illinois at Urbana- Champaign with expertise in the productive performance of pigs. The diet was manufactured at the University of Illinois at Urbana-Champaign feed mill, which is included in the AAALAC accredited program and follows Good Practices for the Feed Industry. All animals were monitored daily, including weekends and holidays, by a trained animal care technician.

ABBREVIATIONS

AST	aspartate aminotransferase
HCC	hepatocellular carcinoma
LRT	locoregional therapy
MRE	magnetic resonance elastography
OCM	Oncopig Cancer Model

REFERENCES

1. World Health Organization. GLOBOCAN 2012: estimated cancer Incidence, mortality and prevalence worldwide in 2012. Available at: globocan.iarc.fr/Pages/fact_sheets_cancer.aspx. Accessed April 24, 2018.
2. Flores A, Marrero JA. Emerging trends in hepatocellular carcinoma: focus on diagnosis and therapeutics. Clin Med Insights Oncol 2014; 8:71–76. [PubMed: 24899827]

3. Rahib L, Smith BD, Aizenberg R, et al. Projecting cancer incidence and deaths to 2030: the unexpected burden of thyroid, liver, and pancreas cancers in the United States. Cancer Res 2014; 74:2913–2921. [PubMed: 24840647]
4. Testino G, Leone S, Borro P. Alcohol and hepatocellular carcinoma: a reviewand a point of view. World J Gastroenterol 2014; 20:15943–15954. [PubMed: 25473148]
5. Tsai MJ, Chang WA, Huang MS, Kuo PL. Tumor microenvironment: a new treatment target for cancer. ISRN Biochem 2014; 2014:351959. [PubMed: 25937967]
6. Avritscher R, Wright KC, Javadi S, et al. Development of a large animal model of cirrhosis and portal hypertension using hepatic transarterial embolization: a study in swine. J Vasc Interv Radiol 2011; 22:1329–1334. [PubMed: 21802316]
7. Schook LB, Collares TV, Hu W, et al. A genetic porcine model of cancer. PLoS One 2015; 10:e0128864. [PubMed: 26132737]
8. Schachtschneider KM, Schwind RM, Darfour-Oduro KA, et al. A validated, transitional and translational porcine model of hepatocellular carcinoma. Oncotarget 2017; 8:63620–63634. [PubMed: 28969016]
9. Dell RB, Holleran S, Ramakrishnan R. Sample size determination. ILAR J 2002; 43:207–213. [PubMed: 12391396]
10. Jackson PGG, Cockcroft PD. Clinical Examination of Farm Animals. Oxford, UK: Blackwell Science Ltd; 2002:198–216.
11. Huang SY, Abdelsalam ME, Harmoush S, et al. Evaluation of liver fibrosis and hepatic venous pressure gradient with MR elastography in a novel swine model of cirrhosis. J Magn Reson Imaging 2014; 39: 590–597. [PubMed: 24532376]
12. Bedossa P, Poynard T. An algorithm for the grading of activity in chronic hepatitis C. The METAVIR Cooperative Study Group. Hepatology 1996; 24:289–293. [PubMed: 8690394]
13. Schneider CA, Rasband WS, Eliceiri KW. NIH Image to ImageJ: 25 years of image analysis. Nat Methods 2012; 9:671–675. [PubMed: 22930834]
14. Linkert M, Rueden CT, Allan C, Burel JM, Moore W, Patterson A, et al. Metadata matters: access to image data in the real world. J Cell Biol 2010; 189:777–782. [PubMed: 20513764]
15. Graudal N, Leth P, Marbjerg L, Galloe AM. Characteristics of cirrhosis undiagnosed during life: a comparative analysis of 73 undiagnosed cases and 149 diagnosed cases of cirrhosis, detected in 4929 consecutive au¬topsies. J Intern Med 1991; 230:165–171. [PubMed: 1650808]
16. Melato M, Sasso F, Zanconati F. Liver cirrhosis and liver cancer. A study of their relationship in 2563 autopsies. Zentralbl Pathol 1993; 139:25–30. [PubMed: 8388716]
17. Scaglione S, Kliethermes S, Cao G, et al. The epidemiology of cirrhosis in the United States: a population-based study. J Clin Gastroenterol 2015; 49:690–696. [PubMed: 25291348]
18. Mokdad AA, Lopez AD, Shahraz S, et al. Liver cirrhosis mortality in 187 countries between 1980 and 2010: a systematic analysis. BMC Med 2014; 12:145. [PubMed: 25242656]
19. Rehm J, Samokhvalov AV, Shield KD. Global burden of alcoholic liver diseases. J Hepatol 2013; 59:160–168. [PubMed: 23511777]
20. Gould SE, Junttila MR, de Sauvage FJ. Translational value of mouse models in oncology drug development. Nat Med 2015; 21:431–439. [PubMed: 25951530]
21. Li X, Zhou X, Guan Y, Wang YX, Scutt D, Gong QY. N-nitrosodiethylamine- induced pig liver hepatocellular carcinoma model: radiological and histo- pathological studies. Cardiovasc Intervent Radiol 2006; 29:420–428. [PubMed: 16502159]
22. Mitchell J, Tinkey PT, Avritscher R, et al. Validation of a preclinical model of diethylnitrosamine-induced hepatic neoplasia in Yucatan miniature pigs. Oncology 2016; 91:90–100. [PubMed: 27305144]
23. Ismail MH, Pinzani M. Reversal of liver fibrosis. Saudi J Gastroenterol 2009; 15:72–79. [PubMed: 19568569]
24. Ellis EL, Mann DA. Clinical evidence for the regression of liver fibrosis. J Hepatol 2012; 56:1171–1180. [PubMed: 22245903]
25. Perez-Tamayo R Cirrhosis of the liver: a reversible disease? Pathol Annu 1979; 14 Pt 2:183–213. [PubMed: 232753]

26. Bataller R, North KE, Brenner DA. Genetic polymorphisms and the progression of liver fibrosis: a critical appraisal. Hepatology 2003; 37: 493–503. [PubMed: 12601343]

27. Wang QB, Zhu H, Liu HL, Zhang B. Performance of magnetic resonance elastography and diffusion-weighted imaging for the staging of hepatic fibrosis: a meta-analysis. Hepatology 2012; 56:239–247. [PubMed: 22278368]

28. Cui J, Heba E, Hernandez C, et al. Magnetic resonance elastography is superior to acoustic radiation force impulse for the diagnosis of fibrosis in patients with biopsy-proven nonalcoholic fatty liver disease: a prospective study. Hepatology 2016; 63:453–461. [PubMed: 26560734]

29. Besa C, Wagner M, Lo G, et al. Detection of liver fibrosis using qualitative and quantitative MR elastography compared to liver surface nodularity measurement, gadoxetic acid uptake, and serum markers. J Magn Reson Imaging 11 28, 2017 https://onlinelibrary.wiley.com/journal/15222586; published online 10.1002/jmri.25911.

30. Yu SC, Hui JW, Hui EP, et al. Unresectable hepatocellular carcinoma: randomized controlled trial of transarterial ethanol ablation versus trans¬catheter arterial chemoembolization. Radiology 2014; 270:607–620. [PubMed: 24126369]

31. Yu SC, Hui EP, Tang P, et al. Transarterial ethanol ablation for unresect- able hepatocellular carcinoma: analysis of clinical and tumor outcomes. J Vasc Interv Radiol 2016; 27:639–649. [PubMed: 26803574]

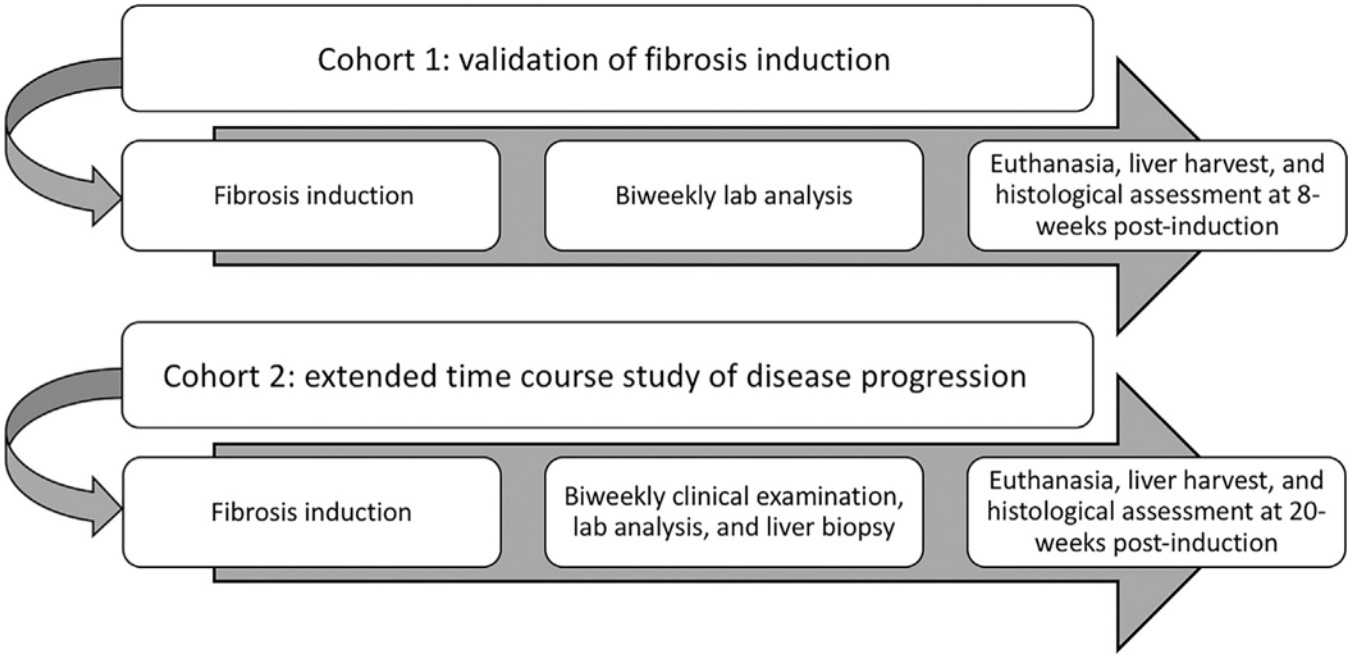

Figure 1.
Flow chart illustrating study design schema. Pathologic outcomes in Cohort 1 were also compared to age- and sex-matched healthy controls.

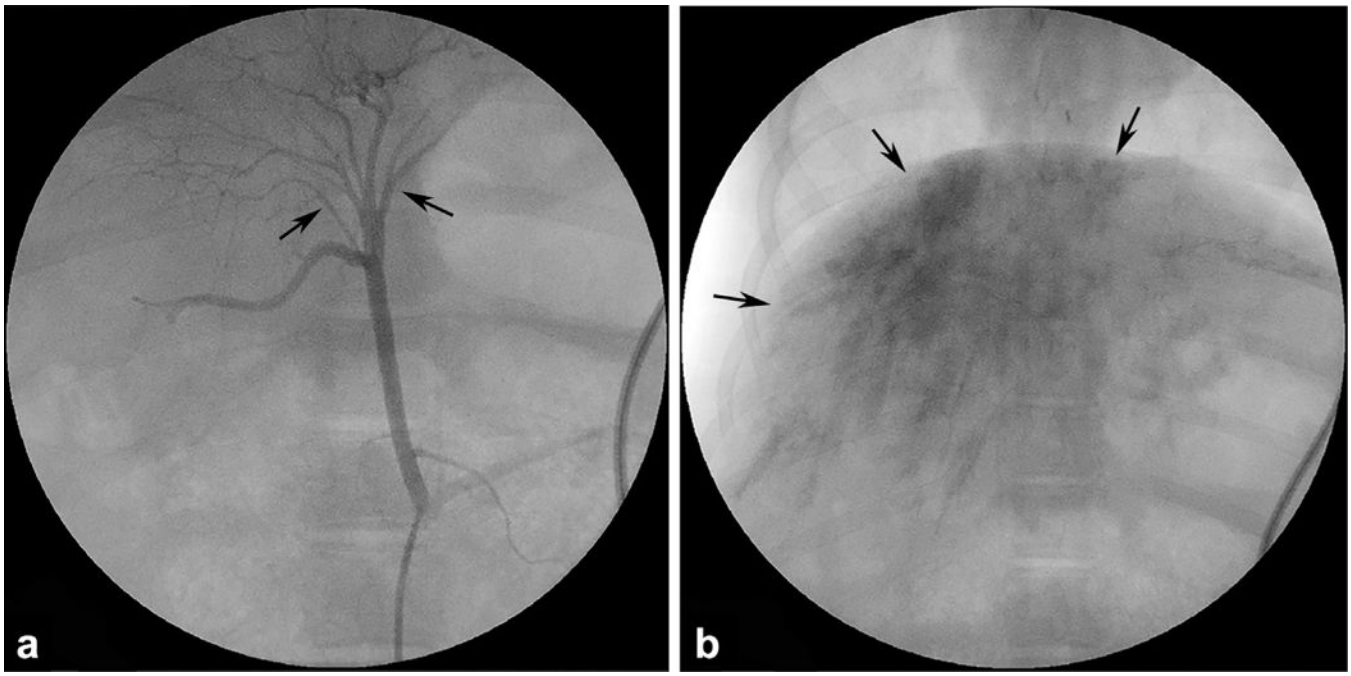

Figure 2.

Representative images from fibrosis induction procedure. (**a**) Celiac arteriogram demonstrates conventional porcine hepatic arteries (arrows). (**b**) Fluoroscopic image obtained after administration of ethanol and ethiodized oil demonstrates deposition of radiopaque emulsion throughout liver (arrows).

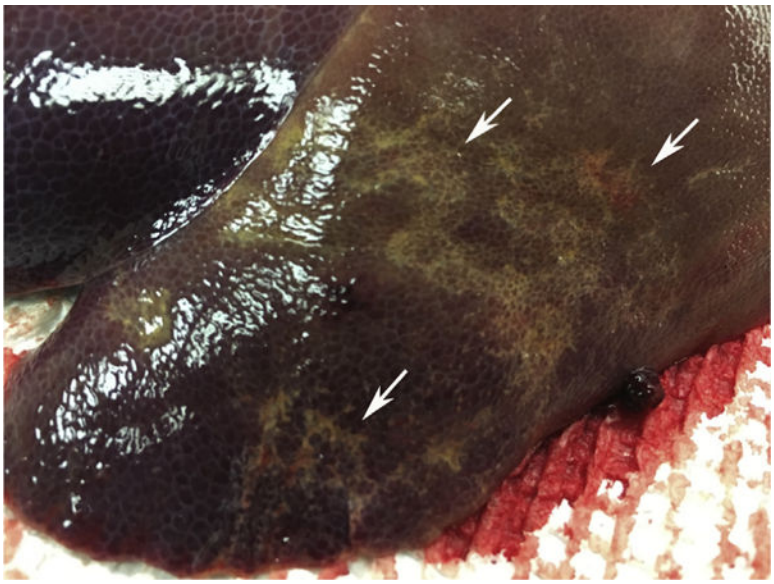

Figure 3.
Gross pathologic photograph of OCM liver 8 weeks after induction demonstrates undulation and nodularity of hepatic capsular surface, as well as enhanced reticular pattern and discoloration (arrows) of hepatic parenchyma, consistent with macronodular fibrosis.

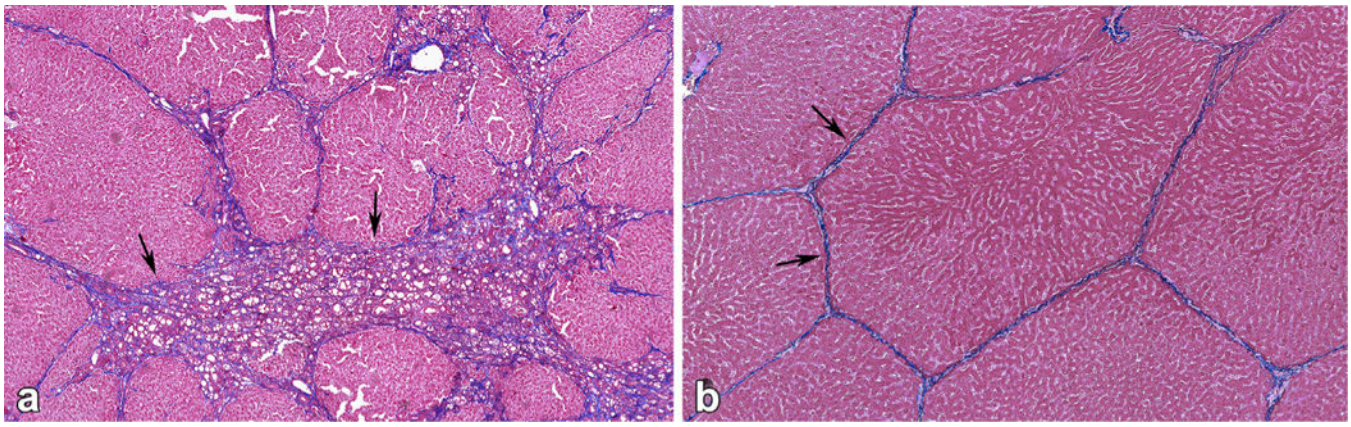

Figure 4.

Representative images of Masson's trichrome-stained Cohort 1 porcine liver sections histologically graded for fibrosis using porcine-adapted METAVIR scheme (all 5x magnification). (**a**) Eight-week post-induction section demonstrating METAVIR F3 fibrosis, with marked expansion of portal areas and fibrous septa by abundant amounts of fibrosis (arrows), which extends into adjacent lobular parenchyma and surrounds and separates hepatocyte clusters. (**b**) Histologically normal porcine control liver with normal pre-existing fibrous septa (arrows), which impart distinct pig liver lobular architecture.

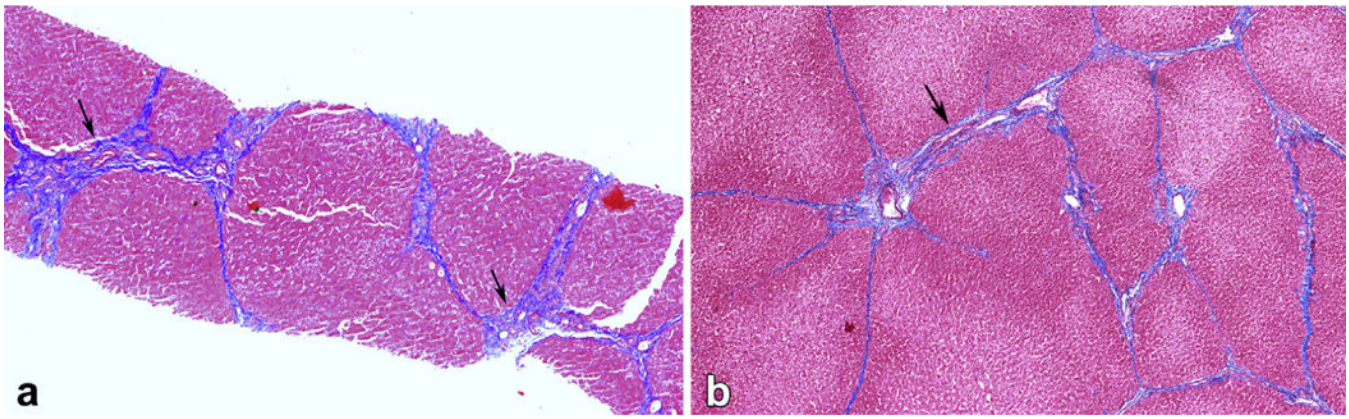

Figure 5.

Representative images of Masson's trichrome-stained Cohort 2 porcine liver sections histologically graded for fibrosis using porcine-adapted METAVIR scheme (all 5x magnification). (**a**) Two-week post-induction section demonstrating METAVIR F2 fibrosis, characterized by moderate fibrous expansion of portal areas and preexisting septa (arrows). (**b**) Twenty-week post-induction section with F2 fibrosis, evident by significant resolution of fibrosis and reestablishment of normal lobular architecture, with only mild fibrous expansion of portal areas and septa (arrow).

Table 1.

Porcine-Adapted Modified METAVIR Fibrosis Grading Scheme

Grade	Description
F0	Normal porcine liver; no increase in fibrosis.
F1	Mild fibrous expansion of portal areas and/or mild thickening/expansion of few random segments of normal preexisting fibrous septa.
F2	Mild to moderate fibrous expansion of portal tracts and multiple, random, noncontiguous segments of normal fibrous septa surrounding multiple hepatic lobules ± presence of thin bands of fibrosis extending from septa or portal tracts into adjacent lobular parenchyma.
F3	Moderate to marked fibrous expansion of contiguous segments of fibrous septa surrounding multiple hepatic lobules; fibrous expansion can involve contiguous segments of septa and partially encircle hepatic lobules but typically does not completely circumscribe lobules. Presence of fibrous connective tissue that dissects into lobular parenchyma, surrounding and separating cords of hepatocytes.
F4	Cirrhosis; normal fibrous septa surrounding hepatic lobules are expanded by moderate to marked amounts of fibrous connective tissue, with some portal bridging, and frequent dissection into adjacent lobular parenchyma, and separation of hepatic cords. Fibrous connective tissue often completely circumscribes multiple hepatic lobules, which appear irregular/shrunken.

Table 2.

Porcine-Adapted Modified METAVIR Inflammation Scoring Scheme

Portal Inflammation/ Interface Hepatitis	Lobular Necro-Inflammatory Foci	Activity Score
None/within normal limits	None	A0
	At least 1 per lobule	A1
	Several per lobule	A2
Mild to moderate	None	A1
	At least 1 per lobule	A2
Moderate with multifocal	None	A2
interface hepatitis	At least 1 per lobule	A3
Moderate to severe with marked interface hepatitis	Any amount	A3

Table 3.

Representative Laboratory Outcomes

	Cohort 1	Cohort 2	Control
Platelets (103/mL)*			
Baseline	512 (457–637)	367 (109–435)	539.5 (488–581)
4 weeks	587 (526–750)	340 (235–397)	531 (367–549)
6 weeks	460 (371–522)	354 (264–377)	528 (444–566)
8 weeks	-	319 (316–377)	-
20 weeks	-	301 (298–352)	-
Total bilirubin (mg/dL)†			
Baseline	0.5 (0.3–0.9)	0.1 (0.1–0.3)	0.1 (0.1–0.2)
4 weeks	0.1 (0.1–0.1)	0.1 (0.1–0.1)	0.1 (0.1–0.1)
6 weeks	0.1 (0.1–0.3)	0.1 (0.1–0.2)	0.1 (0.1–0.5)
8 weeks	-	0.1 (0.1–0.3)	-
20 weeks	-	0.1 (0.1–0.1)	-
Alkaline phosphatase (U/L)‡			
Baseline	217 (200–274)	258 (249–293)	166 (127–196)
4 weeks	174.5 (157–201)	172 (136–215)	159 (155–183)
6 weeks	135 (120–157)	179 (159–232)	146 (106–157)
8 weeks	-	193 (150–234)	-
20 weeks	-	137 (127–148)	-
AST (U/L)§			
Baseline	43 (30–52)	46(29–71)	41 (25–50)
4 weeks	33 (25–34)	28 (24–74)	31 (31 –33)
6 weeks	35 (19–70)	27 (26–182)	40 (26–48)
8 weeks	-	20 (16–24)	-
20 weeks	-	14 (13–18)	-
Albumin (g/dL)‖			
Baseline	3.3 (3.1–3.5)	3.3 (3.2–3.6)	3.5 (3.4–4.1)
4 weeks	3.6 (3.5–3.9)	3.6 (3.2–3.8)	3.7 (3.7–3.9)

J Vasc Interv Radiol. Author manuscript; available in PMC 2019 February 25.

	Cohort 1	Cohort 2	Control
6 weeks	3.5 (3.3–3.8)	3.2 (3.1–3.6)	3.3 (3.1–3.3)
8 weeks	-	3.7 (3.5–3.8)	-
20 weeks	-	3.8 (3.5–4.0)	-
Prothrombin time (s)[¶]			
Baseline	13.0 (12.5–14.2)	11.9 (11.6–13.1)	12.85 (12.6–14.1)
4 weeks	13.1 (12.2–14.4)	12.0 (9.5–13.1)	14.2 (13.2–14.3)
6 weeks	12.65 (12.1–13.2)	12.8 (11.1–13.4)	14.4 (14.2–14.8)
8 weeks	-	13.4 (11.9–13.4)	-
20 weeks	-	11.7 (11.4–13.5)	-

AST = aspartate aminotransferase.

[*] Reference range = 300–600 10^3/mL (8).

[†] Reference range = 0–10 mg/dL (8).

[‡] Reference range = 120–400 U/L (8).

[§] Reference range = 32–84 U/L (8).

[‖] Reference range = 1.9–2.4 g/dL (8).

[¶] Reference range = none available.

Table4.

Cohort 1 Liver Histologic Outcomes

	8-Week METAVIR Fibrosis Grade*	8-Week METAVIR Inflammation Activity*
Subject 1	3	A2
Subject 2	4	A3
Subject 3	3	A2
Subject 4	4	A3
Subject 5	3	A2
Median	3	A2

*Samples obtained via liver tissue harvest.

Table 5.

Cohort 2 Liver Histologic Outcomes

	METAVIR Fibrosis Grade Most Severe*	20-week†	METAVIR Inflammation Activity Most Severe*	20-week†
Subject 1	3 (week 6)	2	A1 (week 2)	A1
Subject 2	2(week 2)	2	A2(week 2)	A1
Subject 3	3 (week 16)	1	A2(week 2)	A1
Subject 4	3 (week 2)	1	A2(week 2)	A1
Subject 5	3 (week 4)	2	A2(week 2)	A1
Median	3	2	A2	A1

*Samples obtained via percutaneous biopsy.

†Samples obtained via liver tissue harvest.